

# Effects of peptizing conditions on nanometer properties and photocatalytic activity of TiO<sub>2</sub> hydrosols prepared by H<sub>2</sub>TiO<sub>3</sub>

Tong-xu Liu<sup>a,b,d</sup>, Fang-bai Li<sup>a,\*</sup>, Xiang-zhong Li<sup>c</sup>

<sup>a</sup> Guangdong Key Laboratory of Agricultural Environment Pollution Integrated Control, Guangdong Institute of Eco-Environment and Soil Sciences, Guangzhou 510650, PR China

<sup>b</sup> Guangzhou Institute of Geochemistry, Chinese Academy of Sciences, Guangzhou 510640, PR China

<sup>c</sup> Department of Civil and Structural Engineering, The Hong Kong Polytechnic University, Kowloon, Hong Kong, China

<sup>d</sup> Graduate School, Chinese Academy of Sciences, Beijing 100039, PR China

Received 27 August 2007; received in revised form 11 November 2007; accepted 12 November 2007

Available online 19 November 2007

## Abstract

TiO<sub>2</sub> hydrosols were prepared from metatitanic acid (H<sub>2</sub>TiO<sub>3</sub>) by chemical precipitation–peptization method under various peptizing conditions. The effects of peptizing conditions on nanosized properties and photocatalytic activity of TiO<sub>2</sub> hydrosols were investigated. The crystal structure, crystallinity, particle size distribution, and transparency (*T*%) of as-obtained hydrosols were characterized by means of X-ray diffraction, transmission electron microscopy, light-scattering size analyzer, and UV–vis transmittance spectra. The results showed that the properties of hydrosols depended on peptizing conditions including a molar ratio of H<sup>+</sup>/Ti, temperature, and solid content. The photoactivity of TiO<sub>2</sub> hydrosols was evaluated in terms of the degradation of rhodamine B (RhB) in aqueous solution, and formaldehyde (HCHO) and methyl mercaptan (CH<sub>3</sub>SH) in gaseous phase. The results showed that increase in H<sup>+</sup>/Ti ranging 0.19–0.75 led to the decrease in particle size and the increase in transparency. With increasing of temperature, particle sizes increased while the transparency and photoactivity decreased steadily when the temperature was higher than 65 °C. The particle size, transparency and photoactivity of the hydrosols hardly depended on solid content when it was not less than 2%. It should be confirmed that the hydrosols with higher crystallinity, smaller particle size and higher transparency could have the higher photoactivity for the degradation of RhB, CH<sub>3</sub>SH, and HCHO. In this study, the optimal peptizing conditions were determined to be H<sup>+</sup>/Ti = 0.75, temperature = 65 °C and solid content = 2–6%.

© 2007 Elsevier B.V. All rights reserved.

**Keywords:** Formaldehyde; Metatitanic acid; Methyl mercaptan; Peptizing conditions; TiO<sub>2</sub> hydrosol

## 1. Introduction

In recent years, titanium dioxide (TiO<sub>2</sub>) as a semiconductor material with lots of advantages, such as photocatalytic activity, anti-corrosion, stabilization of chemical properties, innocuity and so on, has been studied in the field of photocatalytic techniques for wastewater treatment, air purification and functional materials [1–7]. The agglomeration and precipitation of TiO<sub>2</sub> powder particles in aqueous suspension can reduce the active sites on TiO<sub>2</sub> surface and block light penetration into the suspension significantly [8]. It was also found difficult to coat normal TiO<sub>2</sub> powders onto walls, windows, or furniture easily

and durably for air purification. In addition, spraying aqueous TiO<sub>2</sub> powder suspension directly onto the above substrates may change the material colour or reduce the material transparency [9]. On the other hand, some transparent TiO<sub>2</sub> thin films can be easily prepared by a sol–gel process, but a heat treatment at a high temperature of more than 400 °C is required to acquire high crystallinity [10,11]. Therefore, suitable catalysts for indoor air purification need meet several requirements including high photocatalytic activity, high transparency, strong adherence, and ease of coating onto various materials at room temperature with a durable feature.

Aqueous TiO<sub>2</sub> hydrosol prepared at low temperature (<100 °C) has several advantages of (1) finer particle size with more uniform distribution and better dispersion in water; (2) stronger interfacial adsorption ability; and (3) easy coating on various supporting materials [12]. Some researchers

\* Corresponding author. Tel.: +86 20 87024721; fax: +86 20 87024123.  
E-mail address: [cefbli@soil.gd.cn](mailto:cefbli@soil.gd.cn) (F.-b. Li).

used aqueous peroxotitanium acid gel derived from titanium metal [13] or compounds [14] to synthesize peroxy-modified anatase sol under autoclave conditions [15–17]. Others prepared TiO<sub>2</sub> hydrosols by means of chemical precipitation–peptization process at low temperature (<100 °C) using inorganic and organic titanium sources [18–21]. In our previous works, two types of TiO<sub>2</sub> hydrosols were prepared from titanium sulfate (TiOSO<sub>4</sub>) and metatitanic acid (H<sub>2</sub>TiO<sub>3</sub>) by a chemical precipitation–peptization method [22], and it has been found that the TiO<sub>2</sub> hydrosols prepared from H<sub>2</sub>TiO<sub>3</sub> achieved the higher activity for formaldehyde degradation for indoor air purification than other hydrosols [22].

In fact, the photocatalytic activity and transparency of TiO<sub>2</sub> hydrosols depend on a few factors such as their crystal phase, degree of crystallization, and particle size [23]. The hydrothermal treatment of colloidal TiO<sub>2</sub> suspensions provides a facile route to control grain size, particle morphology, microstructures, phase composition and surface chemical properties via adjusting experimental parameters including temperature, pressure, duration of process, concentration of chemicals and pH of solution [24]. Therefore, the above preparing conditions would affect both of the physical properties and photocatalytic activity of the hydrosol. Some studies have investigated the effects of hydrothermal conditions [25,26] and heat treatment [27] on properties and photocatalytic activity of TiO<sub>2</sub> powders. However, only limited studies were conducted on the effect of peptizing conditions on the properties and photocatalytic activity of TiO<sub>2</sub> hydrosol.

In this work, TiO<sub>2</sub> hydrosols were prepared from H<sub>2</sub>TiO<sub>3</sub> by a chemical precipitation–peptization method. The effects of peptizing conditions of TiO<sub>2</sub> hydrosols on their properties and photocatalytic activity were investigated to provide a comprehensive understanding for preparing TiO<sub>2</sub> hydrosol with high activity and also to promote the application in air purification.

## 2. Experimental

### 2.1. Materials

Metatitanic acid (H<sub>2</sub>TiO<sub>3</sub>) containing 51 wt% of TiO<sub>2</sub> was supplied from Panzhihua Iron & Steel Research Institute, China. NH<sub>4</sub>OH, HNO<sub>3</sub>, and other chemicals with analytical grade were obtained from Shanghai Reagent Ltd. The deionized water was prepared by a RO purification system. Degussa P-25 consisting of 80% anatase and 20% rutile was obtained from Degussa AG Company in Germany.

### 2.2. Preparation of TiO<sub>2</sub> hydrosols

TiO<sub>2</sub> hydrosol was prepared by means of hydrothermal process using H<sub>2</sub>TiO<sub>3</sub> as a precursor with the following procedure: 100 g of H<sub>2</sub>TiO<sub>3</sub> was added into 2 L of deionized water, and then stirred continuously to obtain a uniform suspension. Then, diluted ammonia was dropped therein very slowly until the pH value rose above 9. The resulting suspension was stirred continuously for 3 h, and then filtered. The filter cake was washed with the deionized water for several times until no sulfate ion

was present (sulfate concentration was determined by 0.5 M barium chloride solution) and pH value reached at 7. In this way, most impurities were substantively removed from the hydrosol. Finally, the filter cake was mixed with the deionized water to form a uniform solution with a solid content 1–6%. The nitric acid with a concentration of 10% (v/v) was dropped therein to adjust the pH value to be between 1 and 2, with a ratio of H<sup>+</sup>/Ti = 0.19–1.0. The resulting solution was continuously stirred at room temperature for 4 h, followed by stirring and heating at the temperature of 45–95 °C. The hydrosol solution was further peptized for 24 h to obtain the product TiO<sub>2</sub> hydrosol eventually. In this study, three series of TiO<sub>2</sub> hydrosols were obtained under different preparation conditions.

### 2.3. Characterization of TiO<sub>2</sub> hydrosols

To characterize the properties of the as-prepared TiO<sub>2</sub> hydrosols, the titania xerogel powder was prepared through gelation treatment at 45 °C for 24 h. X-ray powder diffraction (XRD) patterns were recorded on a Rigaku D/Max-III A diffractometer at room temperature, operating at 30 kV and 30 mA, using a Cu K $\alpha$  radiation ( $\lambda = 0.15418$  nm). The crystal phases of the TiO<sub>2</sub> hydrosols were identified by comparing diffraction patterns with those on the standard powder XRD cards compiled by the Joint Committee on Powder Diffraction Standards (JCPDS). The crystal sizes were calculated by Scherrer's formula [25,26]. The particle size distributions (PSD) of the hydrosols were directly determined by a light-scattering size analyzer (Beckman N5, USA). The UV–vis transmittance spectra of the hydrosols in the wavelength range of 200–600 nm were obtained using a TU-1801 UV–vis spectrophotometer (Beijing, China). The sol catalysts were examined by transmission electron microscopy (TEM) using a JEOL JEM-2011 microscope operated at 200 kV. TEM samples were prepared by depositing the hydrosol on a copper grid.

### 2.4. Photocatalytic activity measurement

Rhodamine B (RhB) chemical was used as a representative pollutant to evaluate the photocatalytic activity of the hydrosols in aqueous solution, while methyl mercaptan (CH<sub>3</sub>SH) and formaldehyde (HCHO) were also applied to determine the photocatalytic activity of the hydrosols in gaseous phase.

#### 2.4.1. Experiments of RhB photodegradation

The photodegradation of RhB was conducted in a Pyrex cylindrical photoreactor, in which an 8-W UV lamp with the main emission of 365 nm is positioned at the centre ( $I = 1.28$  mW cm<sup>-2</sup>). The photoreactor is surrounded by a Pyrex circulation water jacket to control the temperature during reaction and is covered by aluminum foil to avoid indoor light irradiation. The reaction colloid solution or suspension was formed by adding given dosage of hydrosol or P-25 powder into 250 mL of aqueous RhB solution. Degussa TiO<sub>2</sub> P-25 was used as a reference photocatalyst to compare the activity with TiO<sub>2</sub> hydrosols. In all experiments here the initial concentration of RhB was 10 mg L<sup>-1</sup> and the solid content of TiO<sub>2</sub> was

0.5 g L<sup>-1</sup>. Prior to the photoreaction, the colloid solution or powder suspension was magnetically stirred in the dark for 30 min to establish adsorption/desorption equilibrium. During the photoreaction process, the colloid solution or suspension was irradiated by UV light with constant aeration and magnetically stirring. And at the given time intervals, the analytical samples were taken from the colloid solution or suspension before stored in the dark. The remaining RhB during the photodegradation was determined by a UV–vis spectrophotometer (UV–vis TU-1800, Purkinje General, Beijing) at a wavelength of 553 nm. P-25/RhB suspension samples were centrifuged for 30 min at 4500 rpm before analysis.

#### 2.4.2. Experiments of CH<sub>3</sub>SH photodegradation

The experiments of CH<sub>3</sub>SH photodegradation were conducted in a batch photoreactor with an effective volume of 33.4 L (29 cm (*H*) × 48 cm (*L*) × 24 cm (*W*)), which was made of organic glass and its inner surface was coated with a Teflon film for eliminating adsorption. Inside of the photoreactor, three lamps (Philips, 8 W, 365 nm) were equipped at the upper level as a light source and the TiO<sub>2</sub>-coated substrate was placed on a Teflon film at the lower level horizontally. The distance between the UV lamps and TiO<sub>2</sub> catalyst is 1.5 cm (*I* = 1.65 mW cm<sup>-2</sup>). A sensor of methyl mercaptan (Detcon DM-100-CH<sub>3</sub>SH) was equipped inside the photoreactor to in situ monitor the CH<sub>3</sub>SH concentration during the experiments. This methyl mercaptan analyzer has a monitoring range of 0–100 ppmv with its resolution of ±2%. In these experiments, it took 1–2 h to reach a gas–solid adsorption/desorption equilibrium, and then the lights were turned on. The humidity was controlled at 52 ± 2% with a humidifier before photoreaction. All the experiments were carried out at the temperature of about 28 °C. In each experiment, the dosage of TiO<sub>2</sub> was 0.5 g as a dry weight of TiO<sub>2</sub> sol. P-25 (0.5 g) was first mixed with 20-ml distilled water to make an aqueous suspension. A sheet of filter paper or aluminum foil with an area of 18 cm × 26 cm (1.07 mg cm<sup>-2</sup>) was used as a supporting medium, and the hydrosol or P-25 suspension was dripped on the filter paper. Then the supported catalyst was dried at the temperature of 70 °C for 24 h. Each experiment lasted for 30 min.

#### 2.4.3. Experiments of HCHO photodegradation

The experiments of gaseous HCHO degradation were conducted in a 0.1 m<sup>3</sup> photoreactor made of stainless steel. The reactor was placed in a small chamber where temperature and humidity were well controlled. In this experiment, TiO<sub>2</sub> hydrosol or P-25 suspension was sprayed onto a piece of glass with a total area of 0.05 m<sup>2</sup> (25 cm × 20 cm) with the catalyst loading of 2 mg cm<sup>-2</sup>. The TiO<sub>2</sub>-coated glass sheet was dried in an oven at 65 °C for about 12 h to evaporate the adsorbed water and then cooled down to room temperature before use. The TiO<sub>2</sub>-coated glass sheet film was fixed inside the reactor, and a set of 8-W Philip UV lamps with the main emission peak at 365 nm was placed at 2 cm above the glass sheet (*I* = 1.42 mW cm<sup>-2</sup>). Then a certain amount of HCHO gas was purged into the photoreactor from the standard gaseous HCHO cylinder (Foshan, China).

Table 1

The effects of various peptizing conditions on the nanometer properties of as-obtained hydrosols

Peptizing conditions		Height of A(1 0 1) peak	<sup>a</sup> Crystal size (nm)	<sup>b</sup> Particle size (nm)
H <sup>+</sup> /Ti (molar ratio)	0.19	232	14.4	43.5
	0.25	237	12.3	30.2
	0.50	225	11.6	27.1
	0.75	219	10.9	26.3
	0.88	220	11.0	28.5
	1.00	222	11.6	28.8
<i>T</i> (°C)	45	168	11.6	27.1
	55	201	11.3	26.1
	65	238	11.4	26.3
	75	241	12.7	28.2
	85	239	14.1	38.9
	95	249	15.4	58.3
Solid content (%)	1	258	16.3	35.2
	2	241	12.6	28.4
	3	228	11.8	27.5
	4	227	11.5	26.7
	5	231	11.1	25.8
	6	224	10.9	26.3
P-25		716	35.1	174

<sup>a</sup> Crystal size was calculated from XRD results based on Scherrer equation.

<sup>b</sup> Particle size was average particle size from PSD.

The initial HCHO concentration was kept at 5.5 ± 0.2 ppmv after adsorption/desorption equilibrium in the dark. All the experiments were carried out at 25 ± 1 °C. The humidity was controlled with a humidifier before photoreaction. The analysis of HCHO in the reactor was conducted with a HCHO monitor (Interscan 4160, USA). Each experiment lasted for 3 h.

### 3. Results and discussion

#### 3.1. Crystal and particle properties

Based on the LaMer theory [28–30], there should be two competitive processes of nucleation and crystal growth when a hydrosol is directly synthesized in an aqueous phase. Crystal growth is influenced significantly by various factors, including a molar ratio of H<sup>+</sup>/Ti, temperature and solid content [31–33].

Fig. 1 shows the XRD patterns of the TiO<sub>2</sub> hydrosol samples prepared under various peptizing conditions. The XRD patterns of the sol samples consisted of five distinctive TiO<sub>2</sub> peaks at 25.38°, 37.98°, 48.08°, 54.68° and 62.88°, corresponding to anatase (1 0 1), (0 0 4), (2 0 0), (1 0 5) and (2 0 4) crystal planes (JCPDS 21-1272), respectively. These results indicated that all the samples had anatase structure. The height of A(1 0 1) in Table 1 can denote the degree of the crystalline for various hydrosols. It was shown that their intensity of peak (1 0 1) was nearly at the identical level, indicating that the crystallinity of the as-obtained hydrosols hardly depended on the molar ratio of H<sup>+</sup>/Ti (as H<sup>+</sup>/Ti) and solid content. But the intensity of peak (1 0 1) increased gradually with the increased temperature from 45 °C to 95 °C. The results also suggested that the temperature

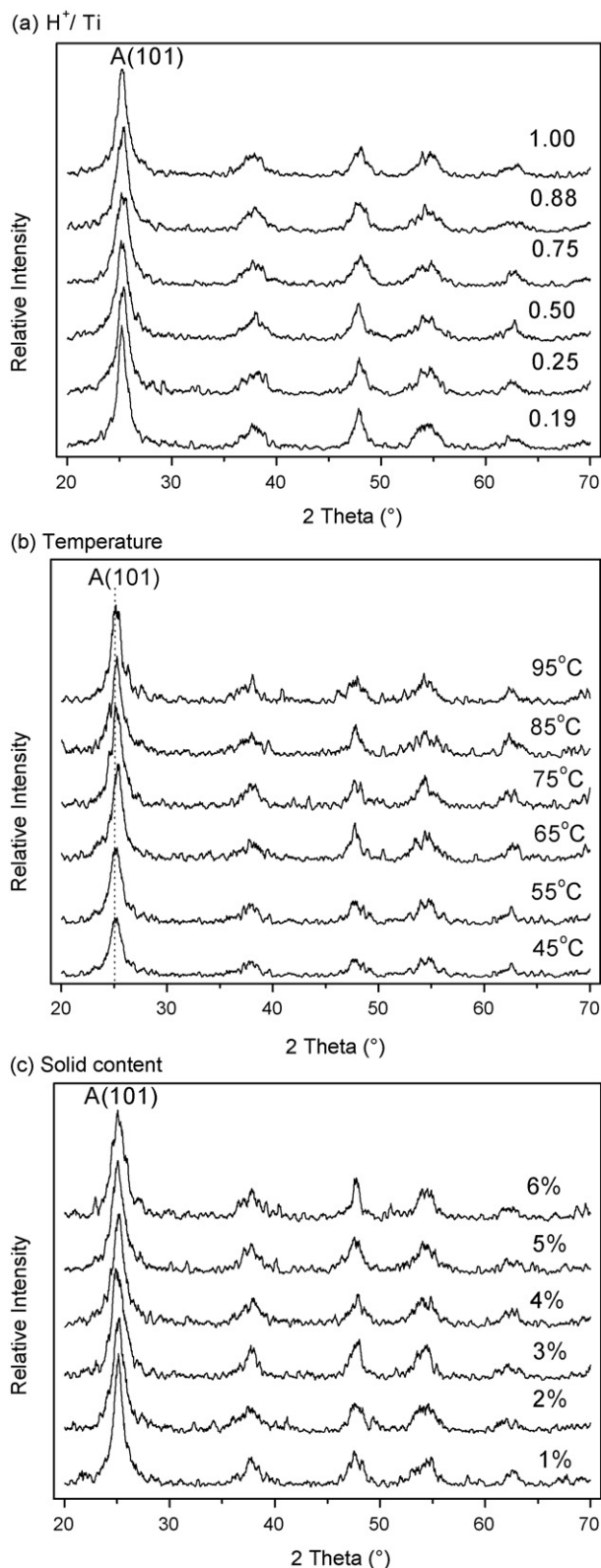


Fig. 1. X-ray diffraction patterns (XRD) of the hydrosol powders with various peptizing conditions: (a) the effect of  $H^+/Ti$  (solid content = 5%,  $T = 65^\circ C$ ); (b) the effect of temperature ( $H^+/Ti = 0.75$ , solid content = 5%); and (c) the effect of solid content ( $H^+/Ti = 0.75$ ,  $T = 65^\circ C$ ).

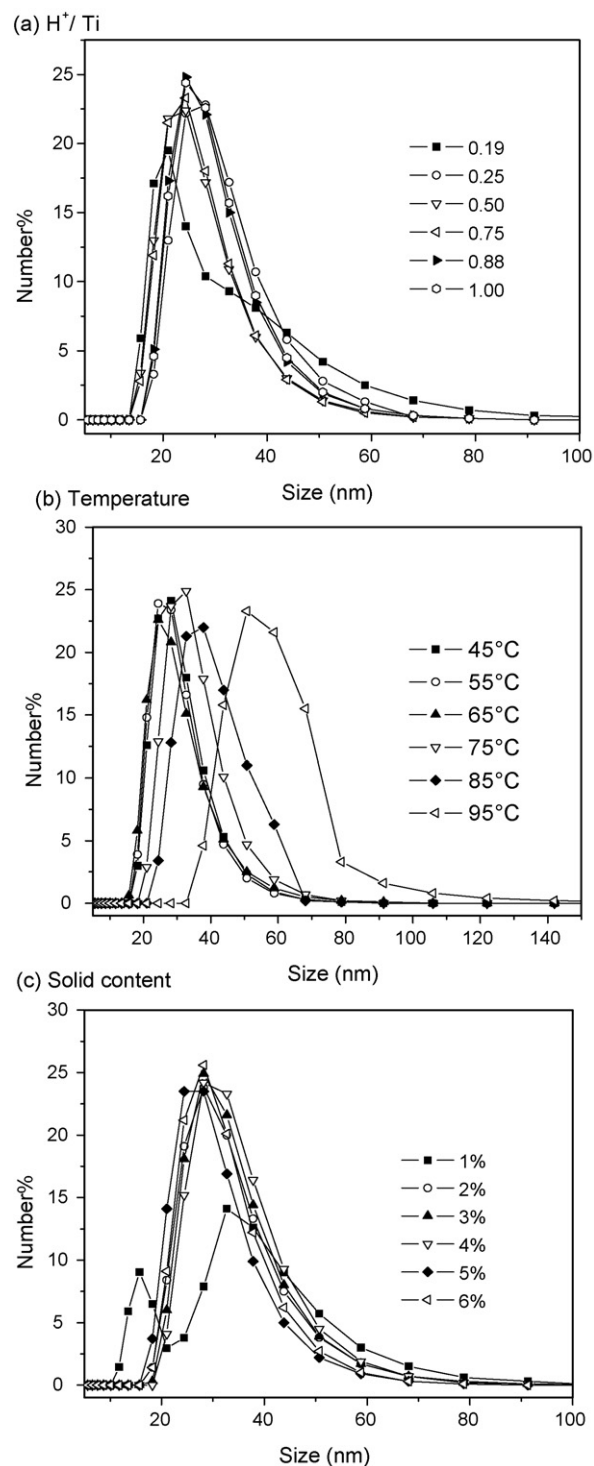


Fig. 2. Particle size distributions (PSD) of the hydrosols with various peptizing conditions: (a) the effect of  $H^+/Ti$  (solid content = 5%,  $T = 65^\circ C$ ); (b) the effect of temperature ( $H^+/Ti = 0.75$ , solid content = 5%); and (c) the effect of solid content ( $H^+/Ti = 0.75$ ,  $T = 65^\circ C$ ).

should be a more significant factor influencing the crystallinity than  $H^+/Ti$  and solid content.

Fig. 2 presented the PSD patterns of the hydrosols prepared under various peptizing conditions. The results showed that the PSD should depend strongly on various peptizing conditions. It was found that the hydrosols with  $H^+/Ti$  0.19 (Fig. 2a) and

the solid content 1% (Fig. 2c) showed multi-modal distributions, while all the other hydrosols had single-modal distribution characteristic with narrow PSD, indicating that the hydrosols were well dispersed in their solutions. Most of particle sizes were distributed in the range of 20–60 nm. In Fig. 2a, there was not remarkable difference among the PSD curves with  $H^+/Ti$  0.25–1.0. In Fig. 2b, it can be seen that the PSD curves shifted significantly to the right as the temperature increased, indicating that the particle sizes of the hydrosols became larger with the increased temperature. In Fig. 2c, the PSD curves of the hydrosols with the solid content of 2–6% were very similar. The competition between the rates of nucleation and crystal growth should affect the PSD modality. The results implied that the rates of nucleation and crystal growth were not very coordinate with  $H^+/Ti$  of 0.19 or solid content of 1%, resulting in the multi-modal distribution. However, the single-modal distribution was obtained in a wide range of peptizing conditions.

To illustrate the trends of changes in crystallinity and particle sizes clearly, the crystallite sizes from XRD results and the average particle sizes from PSD results were calculated and are shown in Table 1. It is clear that the average particle sizes were all much larger than the crystallite sizes due to the slight aggregation of the hydrosol particles, which was mentioned in the previous work [22]. It was shown that the crystallite sizes decreased from 14.4 nm to 10.9 nm as the  $H^+/Ti$  increased from 0.19 to 0.75, and then increased slightly from 0.75 to 1.00. It was found the minimum crystallite size was 10.9 nm with  $H^+/Ti$  0.75. In the meantime, the average particle sizes of hydrosols decreased from 43.5 nm to 26.3 nm as the  $H^+/Ti$  increased from 0.19 to 0.75 and further increased slightly from 0.75 to 1.00. When  $HNO_3$  was added to the amorphous titania hydrates, it could break the oxolation bonds and finally peptize the amorphous precipitate. With increasing  $H^+$  concentration, more oxolation bonds among titanium atoms were broken and the rates of nucleation and crystal growth was changed [34,35]. This also implied that there was an optimal  $H^+/Ti$  (0.75) with the smallest particle size (26.3 nm).

It can also be seen from Table 1 that the crystallite sizes and average particle sizes were all at the same scale with the temperature below 65 °C. As the temperature increased from 65 °C to 95 °C, the crystallite sizes increased slightly, while the average particle sizes increased significantly up to 58.3 nm at 95 °C about twice of that (26.3 nm) at 65 °C. These results indicate that high temperature can accelerate the movement of the hydrosol particles and result in the severe aggregation to increase the particle sizes. It was also found that the crystallite size and particle size of the hydrosol with the solid content of 1% was obviously larger than those with of solid content of 2–6%. If the solid content in the suspension was low, the probability of collision among the hydrosol particles would reduce. The rate of crystalline growth would be faster than that of nucleation, resulted that the anatase crystals grew quickly, and then the particle sizes also became larger. From the results in Table 1, it may be confirmed that the effect of peptizing conditions on the particle sizes was more significant than that on the crystallite sizes, which implies that the phenomena of aggregation is very sensitive to the peptizing conditions.

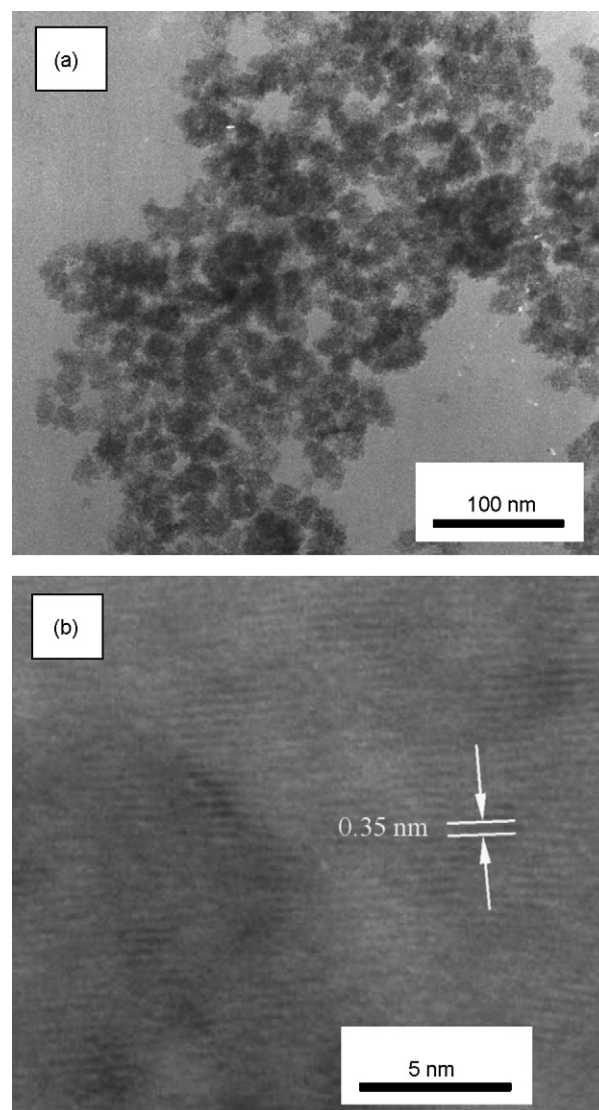


Fig. 3. Transmittance electron microscopy (TEM) (a) and HRTEM (b) of the obtained sol at the following conditions: solid content = 5%;  $H^+/Ti$  = 0.75;  $T$  = 65 °C.

### 3.2. TEM study

Fig. 3a and b shows the TEM and HRTEM images of the  $TiO_2$  hydrosols prepared at the solid content = 5%,  $H^+/Ti$  = 0.75, and temperature = 65 °C. It can be observed in Fig. 3a that the size of the primary particles estimated from the TEM images to be about 20–30 nm, which was in good agreement with the value (26.3 nm) of PSD average size. Fig. 3b shows the corresponding HRTEM image of the hydrosol. The lattice fringes were a little dim, indicating that some amorphous structures on it. But they can still be seen with the fringes of 0.35 nm, which matched that of the (1 0 1) crystallographic plane of  $TiO_2$  anatase.

### 3.3. UV–vis transmittance spectra

Fig. 4a presented the UV–vis transmittance spectra of the hydrosols with different  $H^+/Ti$  ratios. It was found that the transmittances increased greatly as the  $H^+/Ti$  increased from 0.19 to

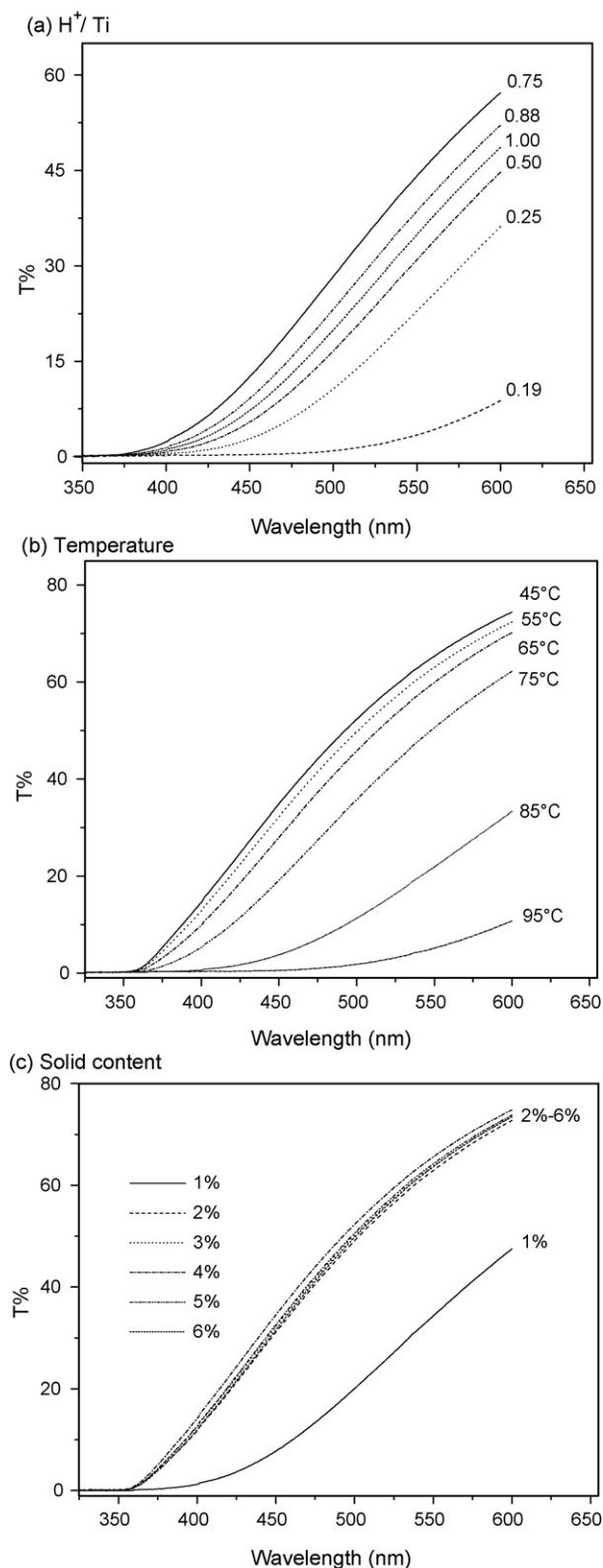


Fig. 4. UV-vis transmittance spectra ( $T\%$ ) of the hydrosols with various peptizing conditions: (a) the effect of  $\text{H}^+/\text{Ti}$  (solid content = 5%,  $T = 65^\circ\text{C}$ ); (b) the effect of temperature ( $\text{H}^+/\text{Ti} = 0.75$ , solid content = 5%); and (c) the effect of solid content ( $\text{H}^+/\text{Ti} = 0.75$ ,  $T = 65^\circ\text{C}$ ).

0.75 and decreased only slightly from 0.75 to 1.00. It has been shown that the maximum transmittance of the hydrosols also had an optimal  $\text{H}^+/\text{Ti}$  ratio of 0.75.

Fig. 4b shows the transmittance spectra of the hydrosols peptized at different temperatures. The transmittance decreased gradually with the temperature increase from  $45^\circ\text{C}$  to  $75^\circ\text{C}$ , but further decreased more quickly from  $75^\circ\text{C}$  to  $95^\circ\text{C}$ . Moreover, it can clearly be seen that the decrements of the hydrosols transmittance had the same trends of particle sizes affected by temperature, which may indicate that the decrease of hydrosols transmittance could result from the increase of particle sizes at the high peptizing temperature.

Fig. 4c shows the transmittance spectra of the hydrosols with different solid contents. The transmittances with the solid content from 2% to 6% had similar values, but much higher than that with the solid content of 1%. These results suggested that the transmittance in general should not depend on the solid content very much as long as beyond 2%. The transmittance property of hydrosols shown in Fig. 4 was well matched with their PSD results. Furthermore, the transmittance property of  $\text{TiO}_2$  thin films should also depend on the transparency of the hydrosols themselves. It is clear that the optical transparency of the  $\text{TiO}_2$  hydrosol thin film is influenced by a degree of colloidal sol dispersion during the peptization process [9]. Therefore, the photocatalytic reaction in the hydrosol system should have a better homogeneity and optical transmittance, compared to that in  $\text{TiO}_2$  powder suspensions [36]. And the hydrosols should be used to prepare the thin films with higher quality such as higher transparency, stronger adherence and less aggregation [37].

### 3.4. Photocatalytic activity

To further investigate the effects of  $\text{H}^+/\text{Ti}$  ratio, temperature and solid content, as three key preparation parameters on the photocatalytic activity of the hydrosols, three sets of experiments were conducted to photocatalytically degrade RhB as a model dye in aqueous solution,  $\text{CH}_3\text{SH}$  as a model odour chemical [38] in gaseous phase and also HCHO as a model air pollutant [39] in gaseous phase. The experimental results are shown in Figs. 5–7, respectively. To compare the reaction rates among the hydrosols, the first-order kinetic constants with the standard deviation were used to fit the experimental data and the kinetic constants ( $k$ ) for various  $\text{TiO}_2$  hydrosols were calculated as summarized in Table 2.

It can be seen that most of the hydrosols had the higher  $k$ -values than that of P-25 powder ( $k = 0.0496 \text{ min}^{-1}$  for RhB,  $0.0538 \text{ min}^{-1}$  for  $\text{CH}_3\text{SH}$  and  $0.4656 \text{ h}^{-1}$  for HCHO), except that the two hydrosols with  $\text{H}^+/\text{Ti} = 0.19$  ( $k = 0.0487 \text{ min}^{-1}$ ) or solid content = 1% ( $k = 0.0295 \text{ min}^{-1}$ ) for the RhB degradation in aqueous phase. In particular, the  $k$ -values for the  $\text{CH}_3\text{SH}$  degradation were even three times higher than P-25. Our previous study [22] suggested that the  $\text{TiO}_2$  hydrosols in comparison with P-25 powder had smaller particle size, more uniform particle size distribution, larger surface area and pore volume, and better transparency. All of these features would contribute to achieve higher photocatalytic activity.

Table 2  
The effects of various peptizing conditions on the first-order kinetic constants ( $k$ ) with the standard deviation for the degradation of RhB, CH<sub>3</sub>SH, and HCHO, respectively

Peptizing conditions	RhB		CH <sub>3</sub> SH		HCHO		
	$k$ (min <sup>-1</sup> )	$R$	$k$ (min <sup>-1</sup> )	$R$	$k$ (h <sup>-1</sup> )	$R$	
H <sup>+</sup> /Ti (mole ratio)	0.19	0.0487 ± 0.003	0.939	0.1417 ± 0.011	0.998	0.6243 ± 0.086	0.840
	0.25	0.0579 ± 0.005	0.900	0.1735 ± 0.015	0.998	0.7395 ± 0.081	0.929
	0.50	0.0634 ± 0.006	0.872	0.1862 ± 0.017	0.998	0.7835 ± 0.075	0.941
	0.75	0.0683 ± 0.005	0.922	0.1887 ± 0.016	0.999	0.7741 ± 0.101	0.893
	0.88	0.0677 ± 0.005	0.917	0.1822 ± 0.015	0.999	0.7483 ± 0.111	0.863
	1.00	0.0562 ± 0.004	0.894	0.1839 ± 0.010	0.996	0.7690 ± 0.089	0.911
$T$ (°C)	45	0.0578 ± 0.004	0.932	0.1497 ± 0.011	0.999	0.6622 ± 0.098	0.813
	55	0.0647 ± 0.005	0.921	0.1824 ± 0.015	0.999	0.7081 ± 0.095	0.865
	65	0.0710 ± 0.004	0.953	0.2035 ± 0.018	0.999	0.7741 ± 0.101	0.893
	75	0.0633 ± 0.004	0.933	0.1962 ± 0.017	0.999	0.7559 ± 0.098	0.893
	85	0.0554 ± 0.004	0.901	0.1747 ± 0.014	0.999	0.7321 ± 0.100	0.873
	95	0.0440 ± 0.004	0.843	0.1762 ± 0.017	0.997	0.7473 ± 0.098	0.892
Solid content (%)	1	0.0295 ± 0.003	0.760	0.1473 ± 0.012	0.998	0.6415 ± 0.081	0.892
	2	0.0605 ± 0.005	0.911	0.1806 ± 0.015	0.999	0.7490 ± 0.097	0.890
	3	0.0645 ± 0.004	0.935	0.1864 ± 0.015	0.998	0.7483 ± 0.111	0.863
	4	0.0591 ± 0.004	0.930	0.1878 ± 0.015	0.998	0.7773 ± 0.107	0.879
	5	0.0727 ± 0.004	0.959	0.1894 ± 0.015	0.998	0.7879 ± 0.101	0.893
	6	0.0684 ± 0.004	0.963	0.1933 ± 0.016	0.998	0.7827 ± 0.099	0.899
P-25		0.0496 ± 0.003	0.974	0.0538 ± 0.019	0.998	0.4645 ± 0.086	0.877

For the RhB degradations, the  $k$ -values of photocatalytic activity of different hydrosols ( $H^+/Ti \leq 0.75$ ) increased with the increased  $H^+/Ti$ , first and then decreased gradually. For the CH<sub>3</sub>SH or HCHO degradation, the photocatalytic activity of different hydrosols ( $H^+/Ti = 0.25-1.0$ ) was found to be similar, which were all significantly higher than that with  $H^+/Ti = 0.19$ . These experiments demonstrated that the photocatalytic activity in gaseous phase was not affected by the  $H^+/Ti$  in the ranged 0.25–1.0 significantly, but when  $H^+/Ti \leq 0.19$ , a significant lower reaction rate was found. From the experimental data in Table 2, the optimal  $H^+/Ti$  ratio may be about 0.75 for all hydrosols.

The effect of peptizing temperature on the photocatalytic activity for degradation of three pollutants demonstrated a similar pattern. All the hydrosols prepared at the temperature of 65 °C showed the highest photocatalytic activity and its  $k$ -values reached 0.0710 min<sup>-1</sup> for the RhB degradation, 0.2035 min<sup>-1</sup> for the CH<sub>3</sub>SH degradation and 0.7741 h<sup>-1</sup> for the HCHO degradation, respectively. This was assigned to the synergetic function of its relatively higher crystallinity, better transmittance, and smaller particle size. The photocatalytic activity of the hydrosols increased with the increase of peptizing temperatures from 45 °C to 65 °C, mainly due to the higher degree of crystallinity from the XRD results. However, when the peptizing temperature was further increased from 65 °C to 95 °C, the photocatalytic activity of the hydrosols decreased gradually, since any further increase of crystallinity from 65 °C to 95 °C was not significant, but the particle sizes increased remarkably, which might lead to the decrement of the activity. Hence, the optimal temperature for preparing TiO<sub>2</sub> hydrosols with the highest activity under this experimental condition would be 65 °C.

The effect of solid content on the photocatalytic activity for degradation of three pollutants also showed a similar trend. Among all the hydrosols with the solid content of 2–6% showed the adjacent photocatalytic activity with the  $k$  values in the range of 0.0591–0.0727 min<sup>-1</sup> for the RhB degradation, 0.1806–0.1933 min<sup>-1</sup> for the CH<sub>3</sub>SH degradation and 0.7483–0.7879 h<sup>-1</sup> for the HCHO degradation, respectively, while all the hydrosol with a solid content of 1% demonstrated much lower activity than others, especially  $k = 0.0295$  min<sup>-1</sup> only for the RhB degradation.

Generally speaking, the hydrothermal treatment can generate the higher hexagonal order and crystallinity of the channels [40–42] and the peptization process can break down the large aggregates into smaller particles by the electrostatic repulsion of the charged particles [9]. It is believed that the transparent hydrosol can easily form clear TiO<sub>2</sub> films with fine size particles uniformly distributed on the supporting medium, which would be the prerequisite for enhancing photoactivity of catalysts [37]. Since the TiO<sub>2</sub> hydrosol can be prepared at a mild temperature condition such as 65 °C with a certain degree of crystallization and good activity, TiO<sub>2</sub> films can be prepared using the hydrosol at room temperature with some advantages over the traditional sol–gel method which needs calcinations at a high temperature such as 450 °C [27].

The above experimental results have well confirmed that the physical properties of TiO<sub>2</sub> hydrosol such as crystal structure, particle size and distributaries, surface area and pore volume can be affected by three key preparation parameters of  $H^+/Ti$  ratio, peptizing temperature and solid content significantly. These physical properties would determine the key features of TiO<sub>2</sub> hydrosol such as the degrees of crystallinity and transparency,

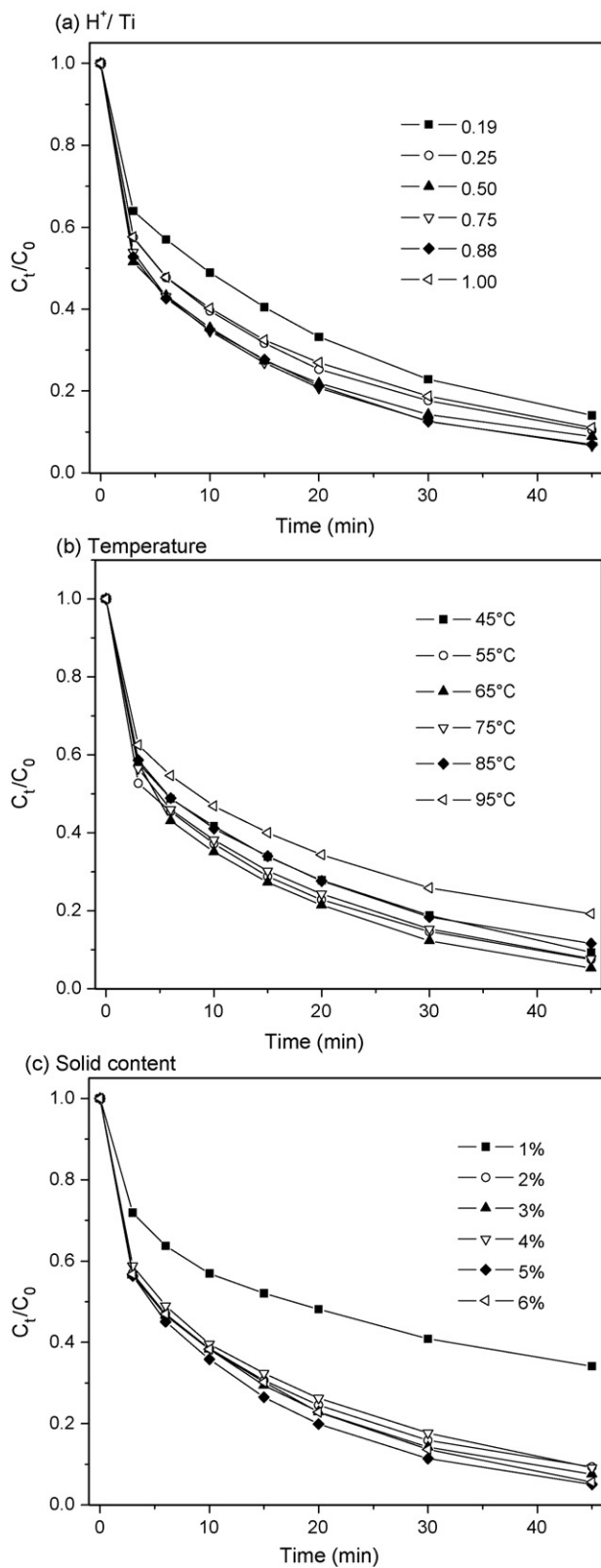


Fig. 5. The RhB photodegradation by the hydrosols prepared under various peptizing conditions under UVA irradiation:  $T = 25 \pm 1^\circ C$ ; the solid content of  $TiO_2 = 0.5 \text{ g L}^{-1}$ ; initial RhB concentration =  $10 \text{ mg L}^{-1}$ ; and reaction time 45 min. (a) The effect of  $H^+/Ti$  (solid content = 5%,  $T = 65^\circ C$ ); (b) the effect of temperature ( $H^+/Ti = 0.75$ , solid content = 5%); and (c) the effect of solid content ( $H^+/Ti = 0.75$ ,  $T = 65^\circ C$ ).

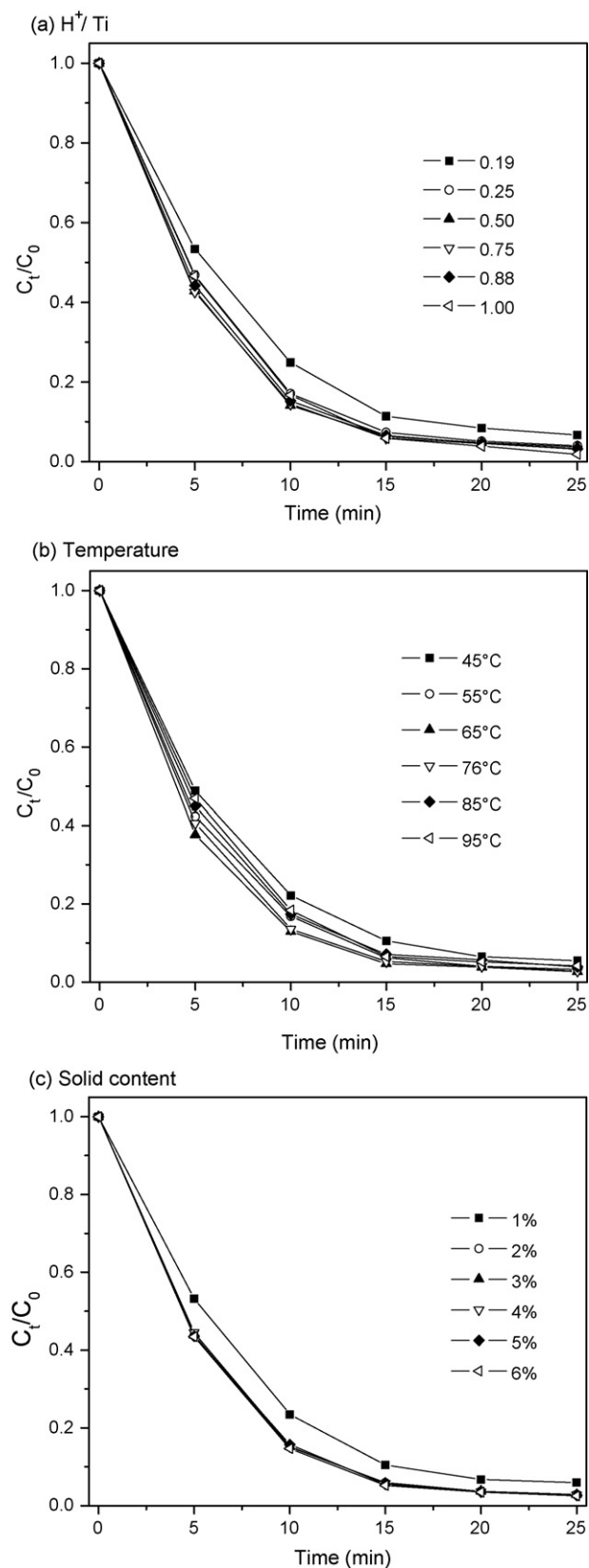


Fig. 6. The  $CH_3SH$  photodegradation by the hydrosols prepared under various peptizing conditions under UVA irradiation: temperature  $25 \pm 1^\circ C$ ; humidity =  $55 \pm 1\%$ ; catalyst loading =  $2 \text{ mg cm}^{-2}$ ; initial  $CH_3SH$  concentration =  $25 \pm 0.5 \text{ ppmv}$ ; and reaction time 25 min. (a) The effect of  $H^+/Ti$  (solid content = 5%,  $T = 65^\circ C$ ); (b) the effect of temperature ( $H^+/Ti = 0.75$ , solid content = 5%); and (c) the effect of solid content ( $H^+/Ti = 0.75$ ,  $T = 65^\circ C$ ).



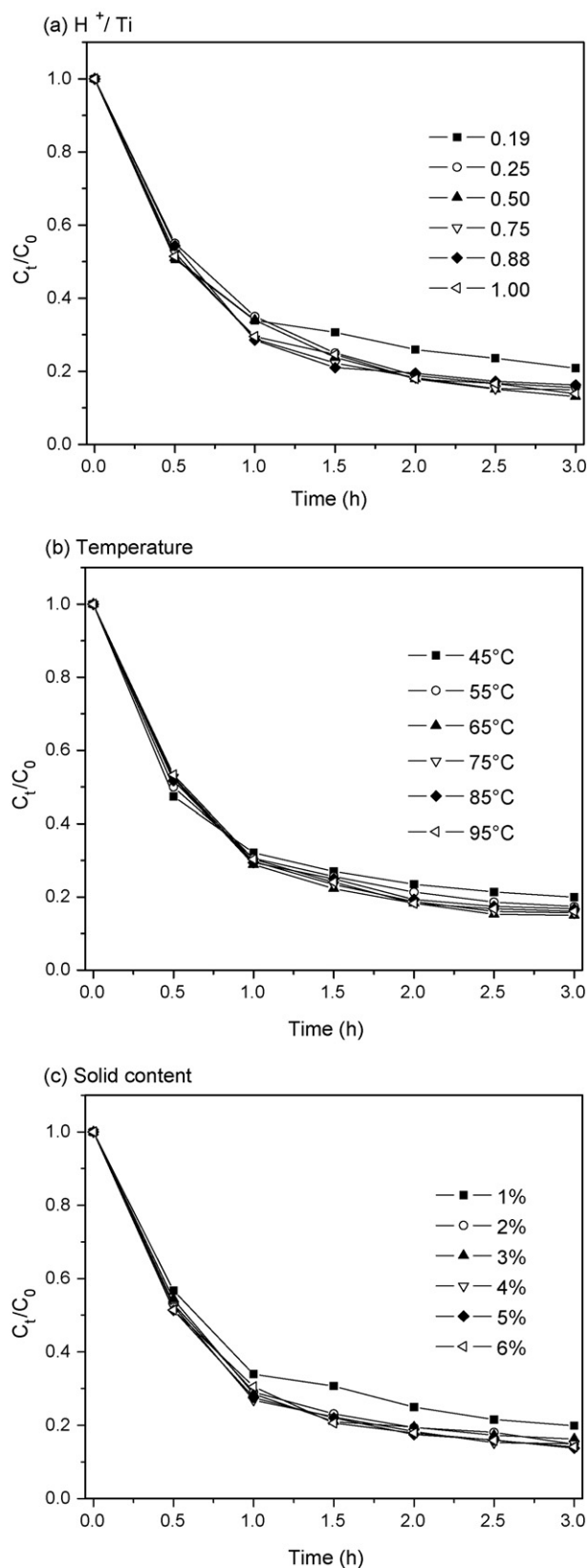


Fig. 7. The HCHO photodegradation by the hydrosols prepared under various peptizing conditions under UVA irradiation: temperature =  $25 \pm 1^\circ C$ ; humidity =  $55 \pm 1\%$ ; catalyst loading =  $2 \text{ mg cm}^{-2}$ ; initial HCHO concentration =  $5.5 \pm 0.2 \text{ ppmv}$ ; and reaction time 3 h. (a) The effect of  $H^+/Ti$  (solid content = 5%,  $T = 65^\circ C$ ); (b) the effect of temperature ( $H^+/Ti = 0.75$ , solid content = 5%); and (c) the effect of solid content ( $H^+/Ti = 0.75$ ,  $T = 65^\circ C$ ).

and eventually influence the overall photocatalytic activity for the degradation of pollutants either in aqueous solution or gaseous phase.

#### 4. Conclusions

$TiO_2$  hydrosols were prepared from metatitanic acid ( $H_2TiO_3$ ) by chemical precipitation-peptization method under various peptizing conditions. The effects of peptizing conditions on nanosized properties and photocatalytic activity of  $TiO_2$  hydrosols were investigated. Three optimal conditions of  $H^+/Ti = 0.75$ , temperature =  $65^\circ C$  and solid content = 2–6% have been determined for preparing  $TiO_2$  hydrosol catalysts with high crystallinity, high transparency and high photoactivity, which have been evaluated in three sets of experiments for the degradation of RhB in aqueous solution,  $CH_3SH$ , and HCHO in gaseous phase.

#### Acknowledgements

The authors are thankful to the RGC grant of Hong Kong Government (RGC Grant No. PolyU5226/06E), and National Natural Scientific Foundation of China (No. 20377011) for financial supports.

#### References

- [1] M.R. Hoffmann, S.T. Martin, W. Choi, B.W. Bahnemann, Environmental applications of semiconductor photocatalysis, *Chem. Rev.* 95 (1995) 69–96.
- [2] A. Fujishima, T.N. Rao, D.A. Tryk, Titanium dioxide photocatalysis, *J. Photochem. Photobiol. C* 1 (2001) 1–21.
- [3] O. Carp, C.L. Huisman, A. Reller, Photoinduced reactivity of titanium dioxide, *Prog. Solid State Chem.* 32 (2004) 33–177.
- [4] X.Z. Li, H. Liu, L.F. Cheng, H.J. Tong, Kinetic behaviour of the adsorption and photocatalytic degradation of salicylic acid in aqueous  $TiO_2$  microsphere suspension, *J. Chem. Technol. Biotechnol.* 79 (2004) 774–778.
- [5] X.Z. Li, H. Liu, L.F. Cheng, H.J. Tong, Photocatalytic oxidation using a new catalyst –  $TiO_2$  microsphere – for water and wastewater treatment, *Environ. Sci. Technol.* 37 (2003) 3989–3994.
- [6] H. Liu, H.T. Ma, X.Z. Li, W.Z. Li, M. Wu, X.H. Bao, The enhancement of  $TiO_2$  photocatalytic activity by hydrogen thermal treatment, *Chemosphere* 50 (2003) 39–46.
- [7] F.B. Li, X.Z. Li, C.H. Ao, S.C. Lee, M.F. Hou, Enhanced photocatalytic degradation of VOCs using  $Ln^{3+}$ - $TiO_2$  catalysts for indoor air purification, *Chemosphere* (59) (2005) 787–800.
- [8] I.K. Konstantinou, T.A. Albanis,  $TiO_2$ -assisted photocatalytic degradation of azo dyes in aqueous solution: kinetic and mechanistic investigations—a review, *Appl. Catal. B* 49 (2004) 1–14.
- [9] H.S. Jung, S.W. Lee, J.Y. Kim, K.S. Kong, Y.C. Lee, K.H. Ko, Correlation between dispersion properties of  $TiO_2$  colloidal sols and photoelectric characteristics of  $TiO_2$  films, *J. Colloid Interf. Sci.* 279 (2004) 479–483.
- [10] N. Negishi, K. Takeuchi, Preparation of a transparent thin-film photocatalyst for elimination of VOC, *Res. Chem. Intermed.* 29 (2003) 861–879.
- [11] S. Park, E. DiMasi, Y. Kim, W. Han, P.M. Woodward, T. Vogt, The preparation and characterization of photocatalytically active  $TiO_2$  thin films and nanoparticles using successive-ionic-layer-adsorption-and-reaction, *Thin Solid Films* 515 (2006) 1250–1254.
- [12] Y.B. Xie, C.W. Yuan, X.Z. Li, Photosensitized and photocatalyzed degradation of azo dye using  $Ln^{(n+)}$ - $TiO_2$  sol in aqueous solution under visible light irradiation, *Mater. Sci. Eng. B* 117 (2005) 325–333.
- [13] P. Tengvall, H. Eluing, I. Lundström, Titanium gel made from metallic titanium and hydrogen-peroxide, *J. Colloid Interf. Sci.* 130 (1989) 405–413.

- [14] R.S. Sonawane, B.B. Kale, M.K. Dongare, Preparation and photo-catalytic activity of Fe–TiO<sub>2</sub> thin films prepared by sol–gel clip coating, *Mater. Chem. Phys.* 85 (2004) 52–57.
- [15] H. Ichinose, M. Terasaki, H. Katsuki, Properties of peroxotitanium acid solution and peroxo-modified anatase sol derived from peroxotitanium hydrate, *J. Sol–Gel Sci. Technol.* 22 (2001) 33–40.
- [16] Y. Gao, Y. Masuda, Z. Peng, T. Yonezawa, Room temperature deposition of a TiO<sub>2</sub> thin film from aqueous peroxotitanate solution, *J. Mater. Chem.* 13 (2003) 608–613.
- [17] L. Ge, M.X. Xu, E. Lei, Y.M. Tian, H.B. Fang, Preparation of TiO<sub>2</sub> thin films using inorganic peroxo titanate complex and autoclaved sols as precursors, *Key Eng. Mater.* 280–283 (part 1–2) (2005) 809–812.
- [18] J. Yang, S. Mei, J.M.F. Ferreira, In situ preparation of weakly flocculated aqueous anatase suspensions by a hydrothermal technique, *J. Colloid Interf. Sci.* 260 (2003) 82–88.
- [19] F. Cot, A. Larbot, G. Nabias, L. Cot, Preparation and characterization of colloidal solution derived crystallized titania powder, *J. Eur. Ceram. Soc.* 18 (1998) 2175–2181.
- [20] D. Lee, T. Liu, Preparation of TiO<sub>2</sub> sol using TiCl<sub>4</sub> as a precursor, *J. Sol–Gel Sci. Technol.* 25 (2002) 121–136.
- [21] Y.B. Xie, C.W. Yuan, Visible-light responsive cerium ion modified titania sol and nanocrystallites for X-3B dye photodegradation, *Appl. Catal. B* 46 (2003) 251–259.
- [22] T.X. Liu, F.B. Li, X.Z. Li, TiO<sub>2</sub> hydrosols with high activity for photocatalytic degradation of formaldehyde in a gaseous phase, *J. Hazard Mater.* 152 (2008) 347–355.
- [23] Y.J. Chen, D.D. Dionysiou, Effect of calcination temperature on the photocatalytic activity and adhesion of TiO<sub>2</sub> films prepared by the P-25 powder-modified sol–gel method, *J. Mol. Catal. A* 44 (2006) 73–82.
- [24] Y.V. Kolen'ko, V.D. Maximov, A.V. Garshev, P.E. Meskin, N.N. Oleynikov, B.R. Churagulov, Hydrothermal synthesis of nanocrystalline and mesoporous titania from aqueous complex titanyl oxalate acid solutions, *Chem. Phys. Lett.* 388 (2004) 411–415.
- [25] J.G. Yu, G.H. Wang, B. Cheng, M.H. Zhou, Effects of hydrothermal temperature and time on the photocatalytic activity and microstructures of bimodal mesoporous TiO<sub>2</sub> powders, *Appl. Catal. B* 69 (2007) 171–180.
- [26] J.G. Yu, Y.R. Su, B. Cheng, M.H. Zhou, Effects of pH on the microstructures and photocatalytic activity of mesoporous nanocrystalline titania powders prepared via hydrothermal method, *J. Mol. Catal. A* 258 (2006) 104–112.
- [27] Y. Tanaka, M. Suganuma, Effects of heat treatment on photocatalytic property of sol–gel derived polycrystalline TiO<sub>2</sub>, *J. Sol–Gel Sci. Technol.* 22 (2001) 83–89.
- [28] V.K. LaMer, R.H. Dinegar, Theory, production and mechanism of formation of monodispersed hydrosols, *J. Am. Chem. Soc.* 72 (1950) 4847–4854.
- [29] T. Sugimoto, Underlying mechanisms in size control of uniform nanoparticles, *J. Colloid Interf. Sci.* 309 (2007) 106–118.
- [30] V.K. LaMer, M.D. Barnes, Monodispersed hydrophobic colloidal dispersions and light scattering properties. I. Preparation and light scattering properties of monodispersed colloidal sulfur, *J. Colloid Sci.* 1 (1946) 71–77.
- [31] I.N. Martyanov, E.N. Savinov, K.J. Klabunde, Influence of solution composition and ultrasonic treatment on optical spectra of TiO<sub>2</sub> aqueous suspensions, *J. Colloid Interf. Sci.* 267 (2003) 111–116.
- [32] J.H. Yang, Y.S. Han, J.H. Choy, TiO<sub>2</sub> thin-films on polymer substrates and their photocatalytic activity, *Thin Solid Films* 495 (2006) 266–271.
- [33] J. Yang, S. Mei, J.M.F. Ferreira, Hydrothermal synthesis of TiO<sub>2</sub> nanoparticles from tetraalkylammonium hydroxide peptized sols, *Mater. Sci. Eng. C* 15 (2001) 183–185.
- [34] R.B. Zhang, L. Gao, Effect of peptization on phase transformation of TiO<sub>2</sub> nanoparticles, *Mater. Res. Bull.* 36 (2001) 1957–1965.
- [35] Y.H. Zhang, G.X. Xiong, N. Yao, W.H. Yang, X.Z. Fu, Preparation of titania-based catalysts for formaldehyde photocatalytic oxidation from TiCl<sub>4</sub> by the sol–gel method, *Catal. Today* 68 (2001) 89–95.
- [36] Y.B. Xie, C.W. Yuan, Transparent TiO<sub>2</sub> sol nanocrystallites mediated homogeneous-like photocatalytic reaction and hydrosol recycling process, *J. Mater. Sci.* 40 (2005) 6375–6383.
- [37] S.Y. Chae, M.K. Park, S.K. Lee, T.Y. Kim, S.K. Kim, W.I. Lee, Preparation of size-controlled TiO<sub>2</sub> nanoparticles and derivation of optically transparent photocatalytic films, *Chem. Mater.* 15 (2003) 3326–3331.
- [38] C.H. Tsai, W.J. Lee, C.Y. Chen, W.T. Liao, Decomposition of CH<sub>3</sub>SH in a RF plasma reactor: reaction products and mechanisms, *Ind. Eng. Chem. Res.* 40 (2001) 2384–2395.
- [39] C. Dimitroulopoulou, M.R. Ashmore, M.T.R. Hillb, M.A. Byrnc, R. Kinnersley, INDAIR: a probabilistic model of indoor air pollution in UK homes, *Atmos. Environ.* 40 (2006) 6362–6379.
- [40] B.M. Wen, C.Y. Liu, Y. Liu, Optimization of the preparation methods synthesis of mesostructured TiO<sub>2</sub> with high photocatalytic activities, *J. Photochem. Photobiol. A* 173 (2005) 7–12.
- [41] J.G. Yu, M.H. Zhou, B. Cheng, H.G. Yu, X.J. Zhao, Ultrasonic preparation of mesoporous titanium dioxide nanocrystalline photocatalysts and evaluation of photocatalytic activity, *J. Mol. Catal. A* 227 (2005) 75–80.
- [42] J.G. Yu, L.J. Zhang, B. Cheng, Y.R. Su, Hydrothermal preparation and photocatalytic activity of hierarchically sponge-like macro-/mesoporous titania, *J. Phys. Chem. C* 111 (2007) 10582–10589.